Dynamics and critical behaviour of neuronal cultures grown on topographical patterns with fractal structure

Author: Mireia Olives Verger*
Master en Física dels Sistemes Complexos i Biofísica.
Facultat de Física, Universitat de Barcelona, Martí i Franquès 1, 08028 Barcelona, Spain.†

Advisor: Jordi Soriano Fradera
(Dated: June 30, 2023)

Neuronal cultures are an excellent experimental tool to study the collective behaviour of neuronal ensembles, providing information on the principles of synaptic functioning and propagation. However, neurons cultured on flat surfaces present limitations in terms of their functionality, as they exhibit a synchronous dynamic behaviour that differs from the much richer repertoire of activity of the brain. In order to address this limitation and help developing better *in vitro* tools to model the brain, here we studied the capacity to break off synchrony by modulating the spatial arrangement of neurons in the substrate they grow. For that, we designed polydimethylsiloxane (PDMS) topographical patterns with fractal geometry and used them as the substrate to grow neurons, with the goal to break the isotropy in connectivity and enrich dynamics. Neuronal activity was recorded with calcium fluorescence imaging and data analysed in the context of criticality, which was inspired by recent findings suggesting that a rich structural connectivity in the brain is behind its functioning at the edge of criticality. We observed that, first, neurons cultured on fractal patterns exhibited richer and more complex dynamics as compared to standard cultures; and, second, that an analysis of the data using the renormalisation group approach, revealed the presence of scale invariance and typical features of systems poised at criticality. Our study is a multidisciplinary endeavour that combined experimental, theoretical and data analysis aspects to validate the hypothesis of the existence of a self-organised criticality in living neuronal networks, from cultures up to the brain.

I. INTRODUCTION

Neuroscience is a constantly evolving scientific discipline whose main objective is to help understanding how the brain works. Modern neuroscience has become so multidisciplinary that it feeds from engineering, physics, mathematics, computer science, and many fields, giving in return new ideas and challenges. Given the sheer size of the brain, neuroscience uses reduced experimental model systems to tackle fundamental questions. One of this models are neuronal cultures, which allow to study the behaviour of nerve cells in a controlled *in vitro* environment [1, 2]. Indeed, neuronal cultures have become a valuable tool for understanding the principles of neuronal functioning and the mechanisms governing the propagation and synaptic transmission of electrical pulses. However, neuronal cultures are still highly limited, and there are still challenges in shaping them as a realistic experimental models that captures the organisational, dynamic and functional aspects of the brain [2].

The present study is an attempt to engineer better neuronal cultures able to display rich, brain-like dynamics. For that, our study aims to modify the substrate in which neurons grow, changing it from Euclidean-like geometry to a fractal one. The idea is to achieve a more intricate connectivity and richer dynamics. Moreover, in this context, experimental, theoretical and data analysis aspects will be combined to validate the hypothesis of self-organised criticality of neuronal dynamics [3]. This hypothesis suggests that the brain exhibits a dynamics in which it approaches a critical state, characterised by a second-order phase transition. In this state, neural activity exhibits critical fluctuations and spatial correlations are established at various scales. This dynamic organisation in the critical state is believed to be optimal for efficient information processing and facilitates adaptation and neural plasticity [4]. In this approach, scale invariance and complex network theory will be fundamental, as they allow the system to be characterised as critical through scaling laws with specific critical exponents.

The present Thesis is organised as follows. In the rest of the section we will introduce fundamental concepts related to neuronal networks and criticality. Then, in the methods sections, we will describe specific experimental and analytical concepts related to our work. We will next describe and discuss the results, analyse the difficulties encountered, and finish with the conclusions.

A. The Brain: Richness, Activity and Connectivity

The brain is a highly complex organ that exhibits a remarkable richness in terms of neuronal activity and connectivity. Within its intricate structure, neurons interact with each other to carry out essential cognitive and behavioural functions, most notably the processing of external information across different brain circuits to understand the environment and take decisions. These

* moliveve10@alumnes.ub.edu
†

functions are based on the electrical activity of neurons and synaptic communication between them.

Under normal conditions, neurons have a negative resting electrical potential, due to the unequal distribution of ions across their membranes. Specifically, the interior of the neuronal cell contains a higher concentration of potassium ions, while the exterior is dominated by sodium and calcium ions. When a neuron receives sufficient stimulation to exceed a certain threshold, a change in membrane permeability to ions occurs. This change leads to the generation of an action potential, also known as *spike*, an electrical signal that travels to other neurons and that represents the basic unit for the transmission and coding of information in neuronal circuits [5–7].

It is important to note that spikes can occur in response to sensory stimuli, cognitive processes, emotions or any other neural activity, as well as from just spontaneous activity, an ubiquitous property of living neuronal networks [8, 9].

Signal transmission.— Neuronal communication occurs through synapses, which allow the transmission of chemical signals known as neurotransmitters from one neuron to another. These neurotransmitters are released by the presynaptic neuron in response to the arrival of an action potential. This action potential induces changes in the membrane potential of the presynaptic neuron, leading to depolarization at the presynaptic terminal. Consequently, voltage-dependent calcium channels become activated, allowing the influx of calcium ions into the presynaptic terminal. The increase in intracellular calcium concentration triggers the fusion of vesicles containing neurotransmitters with the presynaptic membrane. Subsequently, neurotransmitters are released into the synaptic space and diffuse to bind with receptors on the postsynaptic membrane of the receiving neuron, thereby generating a postsynaptic response [5–7]. Interestingly, intracellular Calcium can increase up to 2 orders of magnitude and, thus, by using Calcium indicators one can monitor in the laboratory the dynamics of a neuronal circuit.

Excitatory and inhibitory neurons.— The interaction among neurons can be excitatory or inhibitory, depending on the type of neurotransmitter released at the synapse. Excitatory synapses increase the likelihood of action potential generation in the receiving neurons, thereby promoting neuronal activity. Conversely, inhibitory synapses reduce the probability of action potential generation, suppressing neuronal activity [9]. It is important to note that the interaction between inhibition and excitation plays a fundamental role in information processing in the brain and in the regulation of neuronal activity.

Spontaneous activity.— The brain exhibits as much or more activity when it is in a resting state compared to its activity during the performance of specific tasks [10, 11]. Therefore, neurons not only respond to external stimuli, but also generate patterns of spontaneous activity in the absence of such stimuli. This spontaneous activity plays a fundamental role in various brain functions and is crucial for the formation, survival and refinement of the correct neural circuits [8]. It is actually so important that it is present in any neural network, *in vivo* and *in vitro*. For this reason, it is highly studied in the context of neuronal cultures to understand the fundamental principles governing it [9]. In addition, it has been observed that numerous psychiatric and neurodegenerative diseases are associated with significant alterations in spontaneous activity patterns [10, 12], thus fostering its understanding to treat such diseases.

Connectivity.— Connectivity plays a fundamental role in the organisation and operation of the nervous system, since the distribution of connections describes the circuits of the complex network, whose regions are functionally and structurally interconnected. *Structural connections* correspond to the physical tissue that binds and communicates neurons with each other, while *functional connections* represent topological pathways of correlated activity between active neurons. Indeed, functional links between two neurons have to be understood in a general sense as statistical correlations between their dynamical patterns [13, 14]. Consequently, functional connections are associated with activity interdependencies, in the sense that two neurons that systematically activate together will be strongly functionally linked.

The notion of functionally linked neurons introduces the concept of functional communities or *modules* [15], which are groups of neurons that 'talk' frequently to one another, thus exhibiting a higher internal connectivity as compared to the connectivity with the rest of the network. The modular organisation is a fundamental trait of the brain, and it believed that it enables specialised and efficient processing of information in different cognitive, sensory or motor aspects [16]. Modularity is also linked to the integration-segregation balance, as described next, in the sense that, depending on the number of functional communities, the network can exhibit a higher number of segregated or integrated states.

Integration and segregation.— Integration and segregation are two fundamental concepts in brain organisation. Segregation refers to the functional specialisation of different brain regions. This functional segregation allows for enhanced efficiency in information processing and the execution of specialised tasks within localised communities (Fig. 1A). On the other hand, integration refers to the ability of a neural network to operate as a unified entity, enabling the efficient exchange and processing of information across different brain regions. This allows the integration and coordination of information at multiple levels, which contributes to the performance of

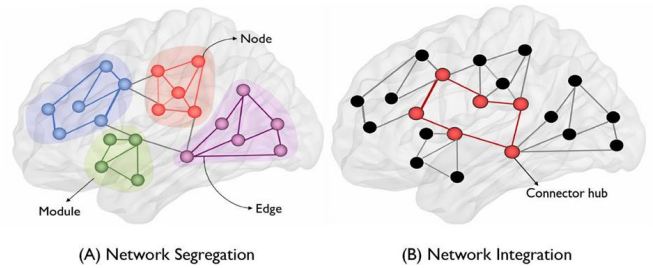

FIG. 1. Schematic diagram showing a set of nodes and edges organised in a network. **A:** Functional segregation indicated by strong functional coupling within communities, represented in different colours, with weak or none functional coupling between communities. This modular organisation allows a specialised computation within each community. **B:** Functional integration indicated by strong functional coupling at the global level, including strong information flow through network centres and their mutual interconnections (red). This phenomenon allows for a global exchange of information.

complex and coordinated cognitive tasks (Fig. 1B) [17–19].

Both integration and segregation are necessary for efficient and adaptive brain processing. Moreover, the neural network of the human brain is characterised by a delicate balance between the two. An excess of integration could lead to a loss of functional specialization and difficulties in the execution of specific tasks. Conversely, an excess of segregation could limit communication between regions and affect the ability to generate adaptive responses. Therefore, an optimal balance between integration and segregation is essential for efficient brain functioning.

In the context of neuronal cultures, the concept of integration-segregation balance is important since standard cultures (grown on a flat Euclidean space) exhibit a highly synchronous, *fully integrated* behaviour that confers them a very poor dynamic repertoire [9, 20]. By tuning the connectivity of a neuronal culture, *e.g.*, through neuroengineering [17, 21], it is possible to escape from such synchronicity and achieve a richer dynamics in which segregation and integration coexist.

B. Brain dynamics as a critical phenomenon

Recent research has revealed the presence of a second-order phase transition in brain dynamics, showing similar characteristics to systems poised in a critical state [3]. As shown in Fig. 2, such a transition separates a disordered or *subcritical* state characterised by random activity, and an ordered or *supercritical* state characterised by persistent highly correlated activity. Near the *critical point*, complexity arises from competition between collective ordering and collective disordering forces, resulting in a state with a wide variety of dynamic patterns [3].

The idea of a continuous phase transition in brain dynamics is related to the brain's ability to simultaneously integrate and segregate information. In the supercritical, ordered state (Fig. 2, yellow square), there is a shared coactivation of activity processes, leading to highly correlated synchronisation states in brain dynamics (bottom-right activity patterns in Fig. 2). In this state, fluctuations have minimal impact on dynamics and the ability to encode information is low. At the other extreme, in the subcritical, disordered state (Fig. 2, red square, and bottom-left activity patterns), more segregation is observed and the system is more responsive to noise and randomness, resulting in weakly correlated dynamics that hinder the flow of information [22, 23]. Hence, the critical point (Fig. 2, blue square and bottom-middle patterns) reflects an optimal balance between segregation and integration in brain behaviour.

Interestingly, the transition point corresponds to a scenario in which the brain exhibits the greatest variability in its repertoire of states. Although the brain fluctuates between subcritical and supercritical states, it has been observed that most of the time the brain remains at the critical transition point. Therefore, the critical state implies a delicate dynamic equilibrium, where neural activity shows critical fluctuations and spatial correlations are established at different scales. Moreover, it produces enhanced functionality in a generic way, which facilitates the task of self-organisation, adaptation and evolutionary mechanisms [23, 24].

A key aspect of a second-order phase transition at criticality is the divergence of a correlation length, which refers to the characteristic distance over which system properties are interrelated. This phenomenon implies scale invariance, which means that activity patterns exhibit the property of self-similarity, repeating the same dynamical traits at different scales, *i.e*, without a dominant characteristic scale [3].

In order to characterise a dynamical system as critical, a classical approach has always been the use of power laws, each with specific critical exponents that satisfy scaling relationships. As predicted by scaling theory [25–27]:

$$f(S) \sim S^{-\tau}, \tag{1}$$

$$f(T) \sim T^{-\alpha}, \tag{2}$$

$$\langle T \rangle(S) \sim S^{\gamma}, \tag{3}$$

where f is the probability distribution function of the associated variable. S and T are, respectively, the size and duration of *avalanches*, *i.e.*, the clustering of groups of consecutive peaks within the whole system. For instance, in the context of Fig. 2, avalanche sizes are the size of collective activations (apparent blue vertical bars in the bottom panels). The parameters τ, α and γ are critical exponents of the system and are related through a scaling relation:

$$\frac{\alpha - 1}{\tau - 1} = \frac{1}{\gamma}. \tag{4}$$

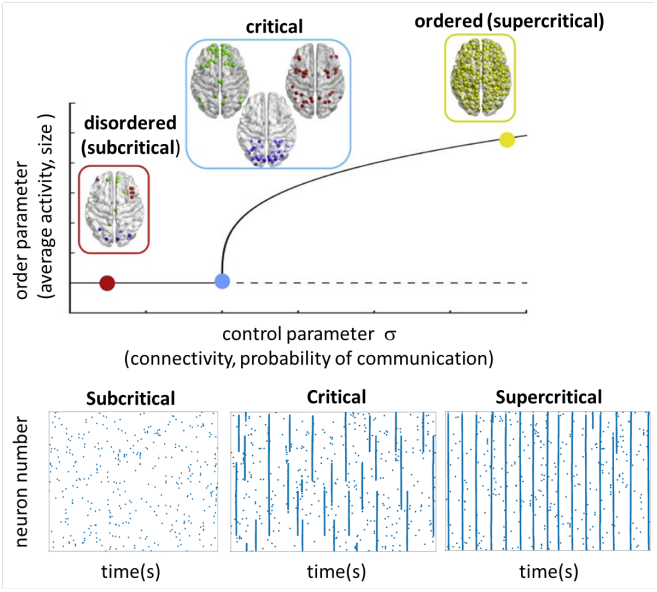

FIG. 2. Proposed role of criticality in large-scale resting-state brain dynamics. In the **subcritical** region, individual brain regions are effectively decoupled, showing a lack of integration (red square). This phenomenon is reflected in the activity patterns of neuronal cultures, which are more asynchronous and irregular because the system is more segregated and random (bottom-left activity patterns). In contrast, in the **supercritical** region, the integration is too large and there is a lack of segregation (yellow square), which causes a large number of neurons to be activated in a short period of time, indicating network bursts, *i.e.*, highly correlated synchronisation states (bottom-right activity patterns). Near the **critical** point, brain systems exhibit a dynamic balance of integration and segregation (blue square), fluctuating between various resting-state networks. In this state, patterns of activity (bottom-middle activity patterns) are characterised by multiple groups of coactivation patterns, establishing spatiotemporal correlations at various scales.

Experimentally, our study investigated criticality using the *group renormalisation approach*, which provides an alternative perspective for characterising criticality in complex systems. In this approach, other quantities are computed, specifically the variance of activity distributions as a function of block neuron size K; the free energy, which is related to the probability that all neurons within a group are in the quiet state; and the covariance matrix spectrum [28, 29]. The scaling exponents corresponding to these quantities were obtained through procedures detailed in Sec. III C, in which hyperscale relationships between them were also established.

C. Neuronal cultures

In 1910 neuroscientist Ross Harrison developed a technique that allowed visualisation and study of live nerve cells *in vitro*, giving rise to the concept of neuronal culture [1, 2]. Neuronal cultures provide a platform for investigating the collective behaviour of neuronal ensembles, enabling a detailed inspection of the principles of neuronal functioning, as well as the mechanisms governing the propagation and synaptic transmission of electrical signals. These cultures have the ability to spontaneously activate and generate various forms of collective spatiotemporal patterns, modelled by network connectivity features and the balance between excitation and inhibition [9, 20, 30]. Moreover, neuronal cultures are ideal systems for manipulation and analysis in the context of complex networks, allowing the extraction of a series of network descriptors or measures that provide information about the statistical properties of the studied network [31]. Therefore, they are particularly relevant for understanding the occurrence of spontaneous activity, the relationship between network dynamics and connectivity, as well as resilience to damage, among other phenomena.

The structure of a neural circuit and its dynamics are closely intertwined, and neuronal cultures can dictate the spatial arrangement of neurons and modulate connectivity across the network based on chemical and/or physical constraints, and combining sophisticated neuroengineering and microfabrication techniques [32, 33]. Such a controlled environment allows the development of models and new network metrics [31], and help the development of new pharmacological agents or therapies [34, 35], altogether aimed at understanding neuronal circuits from a complex system perspective and treat neurological and psychiatric disorders [2]. Therefore, *in vitro* neural networks make possible to study the development of connections in living neural networks and the interplay between connectivity, activity and function. These models provide a solid basis for understanding fundamental mechanisms of neural network dynamics, which can often be extrapolated successfully to the brain.

In terms of physical constraints, it is possible to modify the structure of collective activity by changing the surface on which neural networks are cultured, specifically by including polydimethylsiloxane (PDMS) topographical patterns [21]. In this way, specific structural motifs shape the dynamics and effective connectivity of neuronal cultures, providing connectivity guidance and structural support to neuronal ensembles.

Patterning and connectivity guidance.— In standard cultures on a flat surface, the connectivity between neurons is isotropic and modularity, the central property of brain functional networks outlined above, is rather weak. Moreover, these homogeneous cultures show a strongly synchronous dynamic behaviour with an all-or-none activation patterns [9] (as in the supercritcal regime of Fig. 2) that is considered pathological. In contrast, topographical modelling incorporates guidance of connections, shaping a more anisotropic connectivity that significantly alters the collective behaviour of networks and

enhances the richness of spontaneous activity towards more varied activity events [21], actually as in the critical regime of Fig. 2. This also increases the overall richness of the neural network, generating diverse activity patterns and specific functional connectivity features [21].

However, these topographical structures generate network dynamics that still do not fully resemble *in vivo* brain-like behaviour. Neurons in these structures only connect directionally or along preestablished paths [21], which limits the range of connectivity schemes and network dynamics. To achieve more realistic connectivity patterns and richer dynamics, our present study aims to increase the organisational complexity of neuronal cultures in order to address the structure and dynamics of the brain. Neurons were grown on a substrate composed of valleys and slits with a fractal spatial distribution, and their impact on the overall dynamics of the network was explored. Our hypothesis is that fractal patterns can provide a connectivity and activation structure that allows interaction between groups of neurons at different scales. This can result in richer and more complex dynamics, as interactions between different groups of neurons can generate emergent patterns and non-linear behaviour in the neural network. For the specific case of our work, three different fractal patterns were used, with different heights and levels of fractality: rhombuses, triangles and Sierpinski squares, with heights of 50 and 100 μm.

II. EXPERIMENTAL METHODS

A. Design of fractal patterns

As previously stated, one of the main objectives is to achieve more realistic connectivity schemes and richer dynamics from growing neuronal cultures on a substrate with a fractal geometry. Therefore, in order to obtain PDMS topographical patterns with this arrangement, it was necessary to generate the desired fractal patterns in a vector format, carry out a lithography process and finally elaborate a PDMS mold with topographic patterns.

Fractal patterns in a vector format.— The desired fractal patterns with different orders of fractality were generated from a vector graphics editor (`Inkscape`) and exported as `.svg` format (Fig. 4A). The fractality order refers to the number of iterations performed to generate the fractal structure, which determines the levels of self-similarity observed in the fractal at different scales. A specific example could be the Sierpinski Triangle, whose construction process is illustrated in Fig. 3. In this case, one starts by dividing an equilateral triangle into four smaller triangles and eliminating the central one. This process is repeated iteratively, taking the smaller triangles and dividing them into new sets of four triangles and eliminating again the central ones at each iteration.

To implement these patterns in the photolithography process, it was necessary to reproduce them in a suitable mask. Although there were several options for mask materials, acetate masks were chosen for this work due to their ease of handling and wide availability.

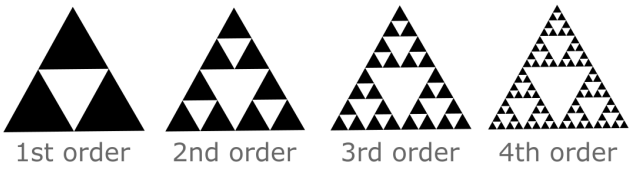

FIG. 3. Sierpinski Triangle construction process.

Lithography process.— The lithography process was carried out in the clean room facilities of the Institute for Bioengineering of Catalonia (IBEC), following a sequence of fundamental steps to obtain the desired patterns on the silicon wafer at a specific height. This height was achieved by uniformly applying thin films of resin on the flat silicon substrate. The choice of resin was based on the target height of the pattern: the resin SO8-3050 was used to achieve a height of 50 μm and the resin SO8-2100 was used to achieve a height of 100 μm. In addition, it should be noted that a shadow transfer method was used during the exposure process, which explains why the objects represented in black in Fig. 4A correspond to the relief areas. The results of this process can be seen in Fig. 4B.

Topographical design with PDMS.— PDMS is a silicon-based organic polymer on which dissociated neurons are seeded. For its production, a mixture of 90% base and 10% curing agent was poured onto the printed circuit board, *i.e.*, the silicon wafer with the fractal patterns relief. Subsequently, the PDMS was cured at 90^{o}C for 2 hours (Fig. 4C). This procedure resulted in the creation of a negative fractal topographic mould of the original design.

B. Neuronal cultures

Preparation of PDMS substrates.— PDMS substrates are widely used in neuronal culture studies due to their mechanical and optical properties, as well as their ability to be chemically modified. Before seeding neurons on PDMS, a preparation process had to be carried out to ensure a suitable surface for neuronal growth.

First, the topographical mould was punctured using a biopsy punch 6 mm in diameter. The mould was then placed on a clean, sterile coverslip and autoclaved in order to sterilise it and promote better adhesion between the PDMS and the coverslip. Next, an oxygen plasma treatment was carried out in order to modify the surface properties of PDMS, which is hydrophobic in its natural state. This procedure led to a hydrophilic

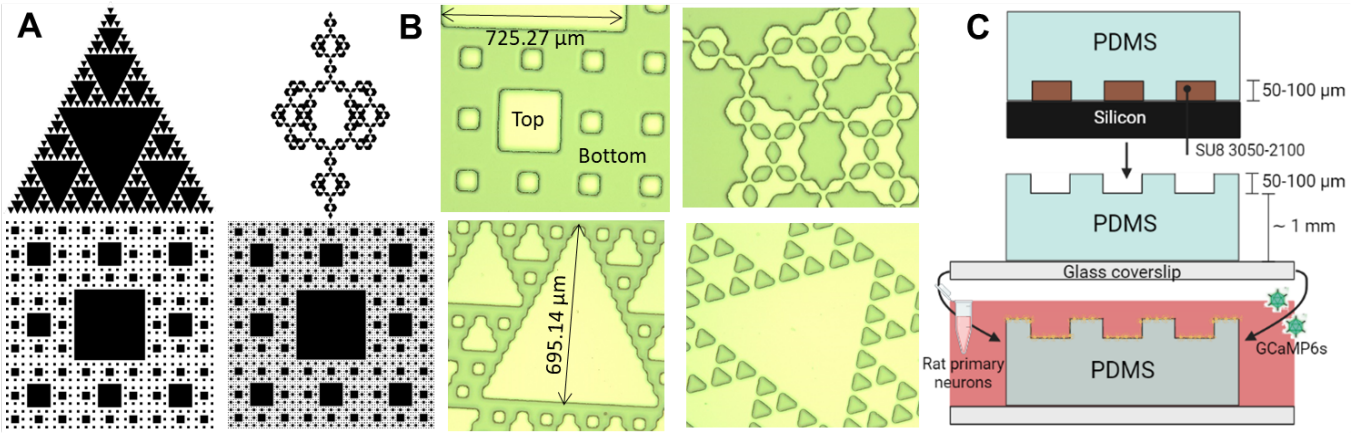

FIG. 4. **A:** Fractal patterns in vector format with different fractality levels, depending on the number of steps used to construct them. The top left figure shows the Sierpinski triangle of order 5, although those of order 6 and 7 were also generated. The top right figure represents a fractal object composed of rhombuses of 3rd order, but 4th and 5th order objects were also generated. The lower figures correspond to the Sierpinski square of order 3 and 4, but that of order 2 was also generated. **B:** Optical microscope images of the silicon wafers with the fractal patterns, which were obtained from a photolithography process. The black objects in figures *A* represent the relief areas with the desired heights (50 and 100 μm), since a shadow transfer method was used in the exposure process. **C:** Sketch of the experimental setup and procedure. A silicon wafer with a topographic relief of 50 or 100 μm height (brown objects in the figure above) was used as a master mould for pouring and curing PDMS. The resulting design corresponds to a reverse-relief replication of the original mould (middle figure). On the PDMS template, neurons were cultured in combination with GCAMP6, which were administered via adeno-associated viruses (bottom figure).

surface that allowed to achieve a more effective coating using a poly-D-lysine (PDL) solution, which favours the adhesion of neurons to the growth surface. As a result, more homogeneous neuronal cultures were obtained.

Preparation of neuronal cultures.— On the day of neuronal seeding, the process was initiated by cleaning the PDL-coated wells with two rinses with sterile distilled water. This was done in order to remove any residual PDL, as its presence is toxic to the cells. Subsequently, the cerebral cortex of rat embryos was extracted and the neurons were mechanically dissociated using an automatic pipette and a thin glass Pasteur pipette. Using this technique, a homogeneous cell suspension containing the individual neurons required for subsequent culturing was obtained.

Then, 1 ml of the resulting cell solution was evenly distributed in each well on the PDMS surface (Fig. 4C, bottom), and the culture plate was placed in the incubator. Usually, half a brain cortex per well was required. However, in the specific case of this work, half a cortex was used for two wells, as the results were better. An example of the obtained networks is shown in Fig. 5A. Control cultures on flat PDMS were also prepared, in order to have an essential reference to monitor the impact of spatial anisotropies on the network dynamics and functional organisation of the neurons.

Transduction of cultures using GCaMP6s.— In order to visualise and monitor neuronal activity in the cultures, the genetically encoded calcium indicator GCaMP6s was used. To achieve this, adeno-associated viruses (AAV) were used to introduce the GCaMP6s gene into the cells. This gene allows the expression of a fluorescent calcium indicator, which facilitates the visualisation of neuronal activity by providing detailed information on changes in intracellular calcium levels. On day 1 *in vitro* (DIV 1), the wells were infected with the adeno-associated viruses, which allowed the neurons to acquire the ability to express the GCaMP6s marker.

Maintenance of neuronal cultures.— To ensure the functionality and survival of the cultures over time, it was necessary to make regular changes to the culture medium to provide essential nutrients, growth factors and supplements. In addition, it was necessary to maintain the cultures in an incubator at 37°C, 95% humidity and 5% CO_2 concentration.

C. Immunostaining

Immunostaining is a widely used technique in neuronal culture studies to visualise and analyse protein expression and cell structure in neuronal cultures. In this project, basic immunostaining was performed on neuronal cultures using a combination of staining with Alexa 488-green fluorescent signal, to identify neurons in the cultures (axons and dendrites); DAPI-blue fluorescent signal, to visualise cell nuclei; and Cell Mask, with red fluorescent signal, to provide a general labelling of cells in the neuronal cultures, including neurons and astrocytes. The latter are specialised cells that support neurons and

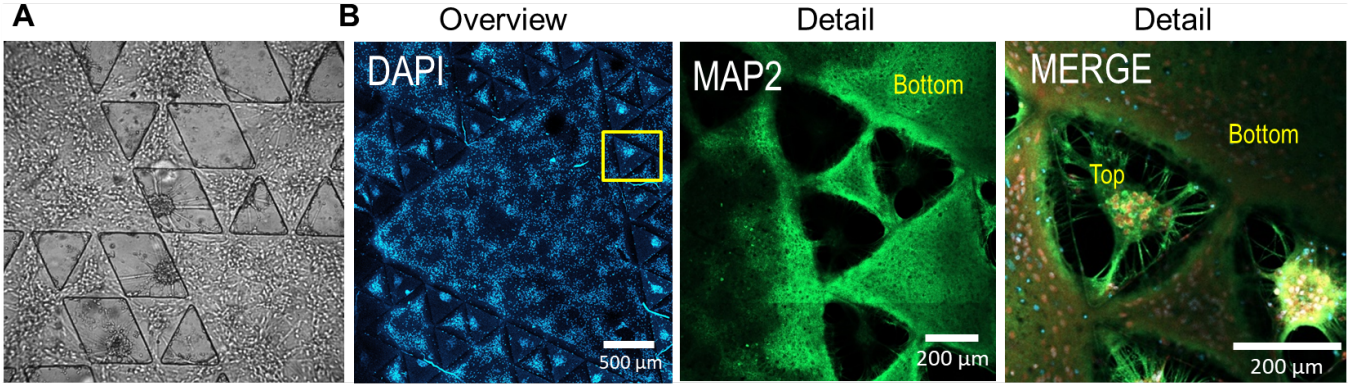

FIG. 5. **A:** Bright-field image of the culture with connectivity directed by a topographical pattern composed of rhombuses. Neurons grow in both the lower and upper regions of the topographic relief, following the shape of the pattern and thereby generating a highly anisotropic circuit. **B:** Immunohistochemical images corresponding to the Sierpinski triangle configuration, with a broad general approach (left) and two detailed approaches (right). These images show cell nuclei in blue (left), dendrites and neuronal processes in green (middle), and the combination of both planes (lower and upper) and channels together with astrocytes in red (right). The yellow square in the figure on the left indicates the part of the culture detailed in the figure on the right.

that are always present in neuronal cultures.

For image acquisition of immunostained samples, a confocal microscope was used to capture the fluorescence signals of specific markers. These images provided detailed information on the location and distribution of the proteins of interest in the neuronal cultures. This information can be obtained in an overview field on the order of mm (Fig. 5B, left) and in detail on the order of μm (Fig. 5B, centre and right). In addition, images were obtained with different focuses (bottom plane and top plane of the culture), channels (green, red or blue) and with the combination of these two effects (focus and channel).

These images showed that neurons were alive and tended to follow the edges of the relief, with some groups of neurons remaining relatively isolated at the top. Therefore, the fractal topography provided some orientation to the connections, resulting in highly anisotropic connectivity.

III. DATA ACQUISITION AND ANALYSIS METHODS

A. Fluorescence calcium imaging

Fluorescence calcium imaging is a fundamental technique to study neuronal activity in neuronal cultures and to better understand the functioning and interaction of neurons in an *in vitro* environment.

The data acquisition process was carried out using an inverted microscope, a specialised camera, a halogen lamp and a blue/green filter for fluorescence excitation/emission. In addition, the Hokawo software was used for image acquisition and control. Thanks to this experimental setup, it was possible to visualise active neurons as bright objects with quasi single-cell resolution, which allowed us to study and analyse their collective behaviour (Fig. 6A). Importantly, measurements of the culture started at DIV 5, at which time the fluorescence signal became strong enough for reliable analysis. Measurements were performed until DIV 18, at which time the neurons began to degrade or detach from the PDMS surface.

B. Measures of interest

Spontaneous activity.— Fluorescence recordings were analysed with the Netcal software [36] run in Matlab. In this process, 732 regions of interest (ROI) were defined in the image (Fig. 6B) and the average fluorescence intensity of each of these regions was extracted over the 15-minute recording duration (Fig. 6C, top). In addition, drifts in the fluorescence traces were corrected and the fluorescence data from each ROI was transformed into time series of neuronal activity using the Schmitt-trigger method. This method considers an abrupt change in fluorescence as an episode of neuronal activity if the fluorescence remains elevated for at least 100 ms between a lower and an upper threshold (Fig. 6C, bottom).

Raster Plot.— Using the time series of neural activity, a raster plot was generated (Fig. 6C, bottom), which allowed the visualisation of the train of activity events detected. This plot was obtained by assigning a value of 1 when the activity of each ROI exceeded a firing threshold at a specific time, and a value of 0 otherwise.

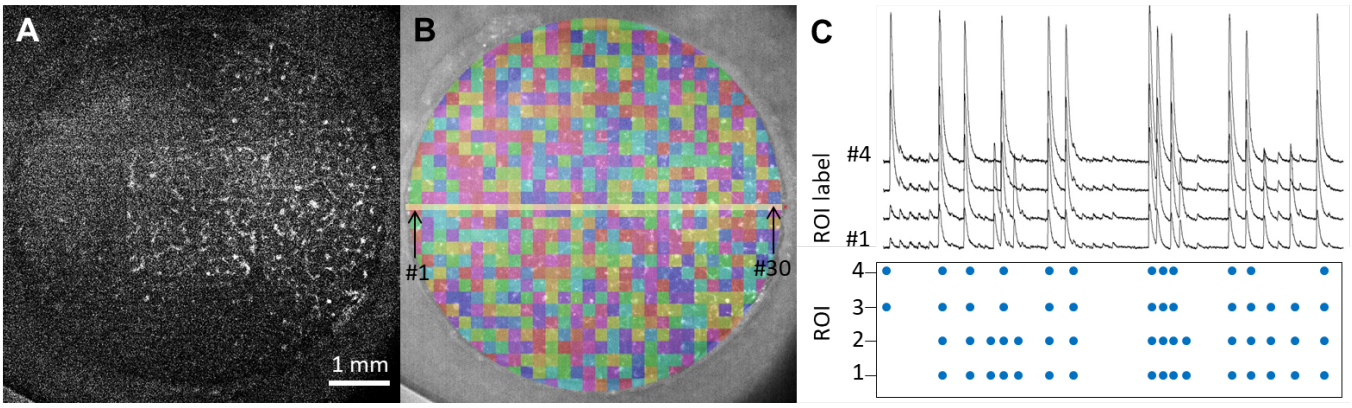

FIG. 6. **A:** Fluorescence images of the topographical design based on the Sierpinski square. Bright dots indicate the presence of active neurons. All cultures analysed were 6 mm in diameter and images were recorded after 6 days *in vitro* (DIV 6). **B:** Regions of interest (ROIs) set as square boxes and covering the entire circular culture, with a total number of 732 ROIs. The labelled ROIs, such as 1 to 30 in the centre of the culture, were used to provide representative fluorescence traces, as shown in the figure on the right. **C:** The upper figure represents the normalised fluorescence traces of 4 ROIs, which have been shifted vertically in order to improve visual clarity. Sharp peaks indicate neuronal activity, which, if it exceeds a firing threshold, its activation time is recorded as a point on the raster plot (bottom figure).

Population activity.— Population activity A quantified the ability of neurons in the network to exhibit coordinated activity, *i.e.*, coordinated activation of a network fraction within a 100 ms window. Population activity was calculated as the proportion of ROIs in the network that activated together without repetition in a sliding window of 1 s width and 0.1 s pitch. Population activity ranged from 0 (no activity) to 1 (full network activation). Sharp peaks in A identified strong coordinated activity and were denoted as *network bursts* [21].

Propagating fronts.— The velocity of the activity fronts was analysed by calculating the Euclidean distance ρ_i from each ROI i to the activity origin (x_0, y_0) and plotting the following ρ_i as a function of t_i' activation times relative to the activity origin [21]. These plots and values for the analysis of the fronts were obtained from software available in Dr. Soriano's lab.

Dynamical richness.— Dynamical richness provides a direct measure for this spatio-temporal variability and reflects the ability of a neural network to exhibit a wide range of dynamic states [17, 37]. It is computed by looking at the distribution of cross-correlation values among all neuronal pairs r_{ij}, *i.e.*, the variability in the behaviour of neurons, allowing to provide a single descriptor, Θ_{CC}, to describe such richness. This descriptor is computed as follows. Following Refs. [17, 37], we first pooled together all CC values r_{ij}, which vary between 0 and 1, and then computed the corresponding distribution $p(r_{ij})$. For example, a completely random dynamics in the network would lead to r_{ij} values close to zero and therefore the distribution $p(r_{ij})$ would have a single peak at zero. At the other extreme, synchronous activity would lead to r_{ij} values close to 1 and the distribution $p(r_{ij})$ would provide a single peak at 1. For rich activity, the distribution $p(r_{ij})$ would be broad. Finally, Θ_{CC} was obtained as

$$\Theta_{\mathrm{CC}} = 1 - \frac{m}{2(m-1)} \sum_{\mu=1}^{m} \left| p_\mu(r_{ij}) - \frac{1}{m} \right|, \qquad (5)$$

where $|\cdot|$ denotes the absolute value and $m = 20$ is the number of bins used for estimating the distributions. Θ_{CC} takes values between 0 and 1, with $\Theta_{\mathrm{CC}} = 0$ for perfectly coherent or random activity, and $\Theta_{\mathrm{CC}} = 1$ for maximally patterned activity, *i.e.*, for a distribution $p(r_{ij})$ that contains all states. In general, the larger Θ_{CC} is, the richer is the dynamics in the culture.

C. Criticality

Brain activity in the context of criticality can be studied using the renormalisation group approach. This makes possible to rationalise collective behaviour at very different observational scales on the basis of the properties of the underlying microscopic components. In addition, it enables the understanding of the emergence of quasi-universal scale invariance in spontaneous neuronal activity [29].

This renormalisation approach aims to group the most correlated neurons, as described later, to identify scalings through power laws, ultimately allowing effective descriptions of time-dependent neuronal activity to be constructed on progressively larger 'coarse-grained' scales. In this context, the rationale of our experiments is to assess whether fractal substrates promote the existence of a scaling behaviour that is absent in flat substrates, thus confirming that rich connectivity is associated with scale invariance and criticality. In addition, the scaling

exponents obtained from neuronal cultures can be compared with those obtained from electrophysiological data of different brain regions in mouse [29], which helps to validate whether our *in vitro* preparations are adequate models for the brain.

On the other hand, one can find evidence that the scale invariance in neuronal activity stems from critical dynamics at the edge of instability, due to a number of non-trivial features typically associated with scale-invariant critical systems. These features include a non-Gaussian distribution of large-scale neural activity; a non-trivial scaling of activity variance and autocorrelation time as a function of coarse-scale granularity; and a power-law decay in the covariance matrix spectrum, suggesting the existence of a scale-free hierarchical organisation of spatio-temporal correlations.

To analyse the data in the context of criticality, the renormalisation group approach was applied using a pairwise maximum correlation criterion to sequentially cluster pairs of neurons. This required the choice of an appropriate discrete time interval for each data set. In this way, the activity time series of the two most correlated neurons were summed up and normalised as described in Ref. [29], resulting in effective time series for 'block-neurons' or simply 'clusters' of size $K = 2^{k=1} = 2$. The process was then repeated with the next most correlated pair of neurons until all neurons were grouped into pairs. Each pair of neurons shaped a cluster (Fig. 7, middle). The next grouping consisted in looking at the most correlated cluster pairs of this construction, leading to a new group of clusters with $K = 2^{k=2} = 4$ (Fig. 7, right). This process was iterated recursively, so after k coarse granularity (RG) steps, $N_k = N/2^k$ block neurons remained, each representing the activity of $K = 2^k$ individual neurons.

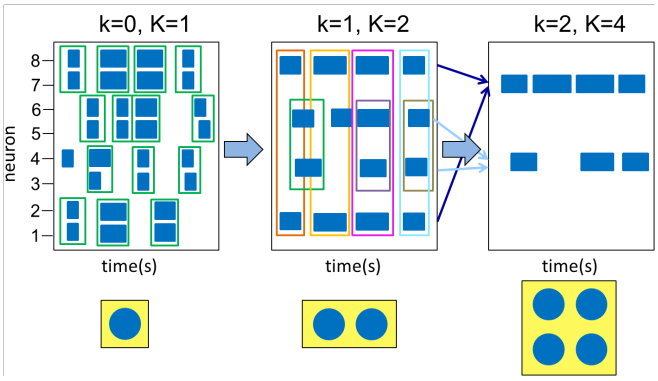

FIG. 7. Scheme of group renormalisation from neuronal activity, where each blue rectangle represents the activity of the neuron that exceeds a certain firing threshold in a given time. The most correlated neurons (and subsequently clusters) are grouped together. k is the number of renormalisation steps and K is the cluster size, *i.e.*, the number of neurons it encompasses.

Then, different quantities of interest were derived from this data [11, 28, 29, 38]:

1) Variance of the activity distributions as a function of the size of K block neurons:

$$M_2(K) = \frac{1}{N_k}\sum_{i=1}^{N_k}\left[\left\langle\left(\sigma_i^{(k)}\right)^2\right\rangle - \left\langle\left(\sigma_i^{(k)}\right)\right\rangle^2\right], \qquad (6)$$

where $\sigma_i^{(k)}$ is the summed activity of the original variables within the cluster.

For fully independent variables, the variance is expected to grow linearly in K, *i.e.*, $M_2(K) \propto K$, while for perfectly correlated variables it grows as $M_2(K) \propto K^2$. Therefore, the non-trivial scaling is characterised by $M_2(K) \propto K^\alpha$ with a certain intermediate value of the exponent $1 < \alpha < 2$.

2) Free energy for coarse-grained variables:

Assuming that the energy of the system is zero when no activity is present, *i.e.*, time frames in which all signals within a cluster are below their activation threshold, the probability of having "silent" block neurons ($\sigma_i^{(k)} = 0$), termed P_{silence}, can be related to the effective free energy of the system as:

$$F(K) = log(P_{\text{silence}}). \qquad (7)$$

As more and more of the initial variables σ_i are grouped into cluster variables $x_i^{(k)}$ (activity of the block-neuron i at step k of the coarse-graining), one would expect that P_{silence} decreases exponentially with the size K of the clusters, leading to: $F(K) \propto K^\beta$ where $\beta = 1$ for initially independent variables and $\beta = 0$ for perfectly correlated variables.

3) Scaling of the covariance matrix spectrum:

It was obtained by diagonalising the calculated covariance matrix at different coarse-grained levels, allowing us to analyse how its decomposition of spectra corresponded with the range of eigenvalues and how its cut-offs changed with the size of the cluster. In this way, the eigenvalues of the covariance matrix scale as:

$$\lambda_r \sim r^{-(2-\nu)/d}, \qquad (8)$$

where r is the rank of λ_r, ordered from the highest to the smallest. If variables within clusters are considered at each coarse granularity step, the highest possible rank r will be given by the number of variables K that make up each cluster. Therefore, at criticality, we should expect:

$$\lambda_r \propto \left(\frac{K}{r}\right)^\mu, \qquad (9)$$

with $\mu = (2-\nu)/d$ as a direct consequence of the power-law decay of the correlation function in space.

One of the hyperscale relationships that can be established between these exponents is based on the contact

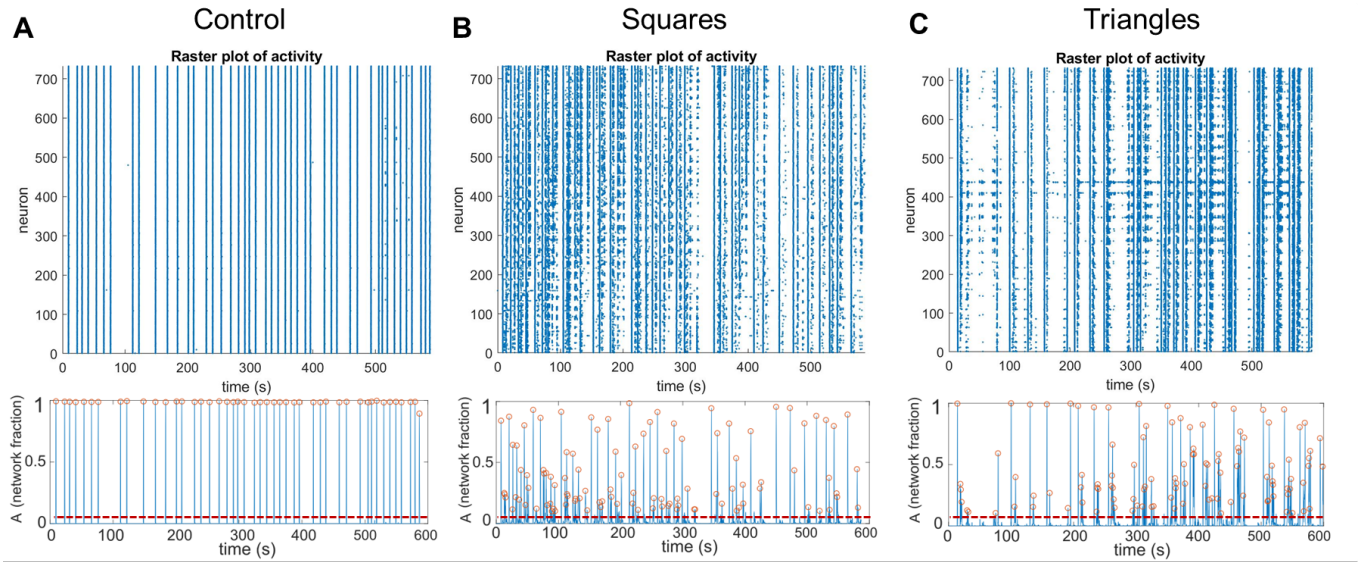

FIG. 8. Above the raster plots and below the corresponding population activity A are represented for the control case (**A**), the Sierpinski square of 4th order (**B**) and the Sierpinski triangle of 5th order (**C**) in young cultures (DIV 6). Population activity captures the fraction of the network that is consistently activated in a short time window. Events that spanned more than 10% of the monitored regions of interest (ROIS) (red dashed lines) were considered significant (orange dots) and formed network bursts of size A.

process, which is a continuous-time Markov process in a network:

$$\eta = d - 2 + \frac{\beta}{\nu_\perp}, \tag{10}$$

where $\nu_\perp = \beta/\alpha$ and $\mu = (2-\eta)/d$.

IV. RESULTS & DISCUSSION

A. Spontaneous activity in neuronal cultures

The collective behaviour of the neuronal cultures was quantified by recording the spontaneous activity in each configuration for 15 minutes, as explained in Sec. III A. In this way, from the generated raster plots, the temporal pattern of neuronal activation and the spatiotemporal organisation in neuronal dynamics can be observed in each specific case.

As shown in Fig. 8A, top panel, activity in the control cultures was characterised by episodes of highly synchronous behaviour in which all ROIs were activated together, having network bursts of the same size (Fig. 8A, bottom) and remained practically silent in between bursts. Therefore, these cultures had an on-off behaviour, which differs significantly from real brain dynamics. By contrast, the Sierpinski square and triangle configurations, showed a much richer dynamic repertoire, in which network bursts of different sizes coexisted (Figs. 8B and 8C) and there was abundant sporadic activity outside these bursts, resulting in a highly rich raster plot.

The network burst sizes were reflected in the population activity, which counts the fraction of ROIs that coactivate together. In Fig 9, it can be seen that all events in the control cultures exhibited sizes $A = 1$, while for the fractal cases the event sizes varied richly from $A \geq 0.1$ to $A \simeq 1$ in both cases. The mean population activity was $\langle A \rangle \simeq 0.4$ in the Sierpinski square case, and $\langle A \rangle \simeq 0.45$ in the Sierpinski triangle case, much lower than in controls, and with a standard deviation of 0.5 and 0.4, respectively, that indicates high variability.

The variety of activity patterns reflected both in the structure of the raster plots and in the distribution of the A values can be quantified through the parameter $\Theta_{\rm CC}$. For the control cases this parameter took values of $\Theta_{\rm CC} \simeq 0.10$, while for the Sierpinski square and triangle this value was $\Theta_{\rm CC} \simeq 0.47$ and $\Theta_{\rm CC} \simeq 0.58$ respectively. Therefore, the fractal cultures clearly exhibited a richer variability in activity patterns.

This analysis was repeated for different configurations, with different levels of fractality, and for all cases similar results were obtained when the cultures were young, between 5 and 7 DIV. However, for mature cultures (DIV 12), the results were similar to the control case due to the ever growing connections in the network over time and that ultimately strongly link the entire culture. In this way, the distributions of collective activations shifted towards higher A values, especially in the case of the Sierpinski square. We note that the development of cultures is complex. The change in dynamics with culture maturation is associated with stronger overall interconnectivity in the network and longer average axons, leading to the formation of neuronal aggregates and long range

connections. These connectivity changes smoothed out the impact of topography on dynamics and favoured a greater presence of bursts throughout the network, becoming a more coordinated and synchronous system.

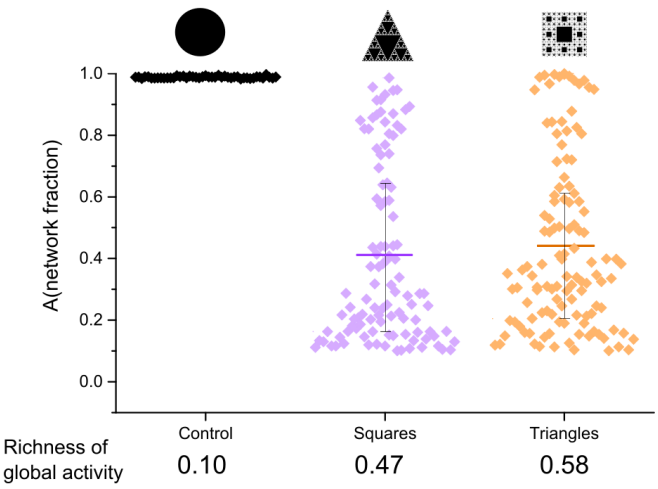

FIG. 9. Distribution of the burst sizes A for the control case, the Sierpinski square of 4th order and the Sierpinski triangle of 5th order in young cultures (DIV 6), with their mean value and standard deviation. In the lower part of the figure, the values of the dynamical richness of the global activity Θ_{CC} corresponding to each of the configurations are shown. The dynamical richness of the global activity represents the variability among the activity patterns of firing neurons, and its value is $\Theta_{CC} = 1$ for maximally patterned activity, and $\Theta_{CC} = 0$ for perfectly coherent or random activity.

B. Repertoire of spatio-temporal activity patterns

The spatio-temporal structure of the bursts in young cultures was analysed using colour maps of their evolution in the cultures for different configurations, as illustrated in Fig. 10A. In the control case, the activity propagated in the form of a quasi-circular front that spanned the entire culture and had a common origin in all bursts. This quasi-circular front manifested itself in a gradual colour change (from black to yellow) in the regions of interest (ROI) that were furthest away from the origin of the activity. Consequently, the activation of the whole network and the uniform location of the explosion initiation resulted in a highly rigid system.

On the other hand, different sizes and propagation patterns were observed in the fractal configurations, indicating a rich variability in the burst structures and initiation points. Therefore, not only did the richness of the system increase, but the propagation fronts were no longer circular and adopted serpent-like trajectories. This reflected a high variability in the possible states of the system and a highly anisotropic connectivity under these conditions.

In addition, the propagation velocity of the fronts, which depends on the connectivity and the balance between excitation and inhibition, was investigated in detail. A high propagation velocity indicates a relatively high connectivity and an isotropic system, as the front can move rapidly in either direction. This phenomenon has two implications: a higher density of connections and longer axons. To study this effect, the characteristic propagation velocity was obtained by linear regression, as shown in Fig. 10B. In the control cultures, the measured velocity was approximately $v \simeq 32$ mm/s, while in the cultures with fractal patterns (Sierpinski square and triangle) it decreased substantially to approximately $v \simeq 14$ mm/s and $v \simeq 8$ mm/s, respectively. This indicates that the presence of patterns in the cultures results in slower propagation velocity, due to the anisotropy of the system and trapping of axons within the fractal motifs, which makes difficult for neurons to extend long axons and connect abundantly with each other, which on average reduces propagation velocities.

Finally, this velocity analysis was completed by comparing the propagation velocities of all fronts for the three configurations, as shown in Fig. 10C. A remarkable lower velocity, by a factor 5, was observed in the data for the Sierpinski square and triangle as compared to controls. Indeed, the velocities differ significantly, as in the control case, the velocity was approximately $\langle v \rangle = 32 \pm 8$ mm/s, whereas in the case of the Sierpinski square and triangle, the average velocities were $\langle v \rangle = 6 \pm 5$ mm/s and $\langle v \rangle = 7 \pm 6$ mm/s, respectively. Additionally, for the particular case of the Sierpinski triangles, a large variability in velocities was observed (a broad distribution of values), suggesting abrupt changes in local connectivity across the neuronal culture that could help imprinting a greater dynamical richness.

We remark that the average activity propagation velocities were approximately 5 times lower in the Sierpinski configuration compared to the control, indicating 5 times lower connectivity in fractal cultures. In this way, low connectivity in the network allowed greater autonomy and diversity in the interactions between neurons, creating an environment favourable for the emergence of greater dynamical richness.

C. Criticality

One of the aims of this work was to test for the presence of scale invariance and analysing whether this invariance stems from criticality or not.

First, all quantities of interest, analysed using the renormalisation group approach, were found to follow an almost perfect scaling for the fractal configurations, as shown in Fig. 11AB. This confirms the existence of scale invariance.

Next, the values of the exponents of the quantities of interest were examined, as well as the autocorrelation and pairwise distribution of covariance values. The variance $M_2(K)$ of the unnormalised activity of block neurons and free energy (Fig. 11A) were found to scale with expo-

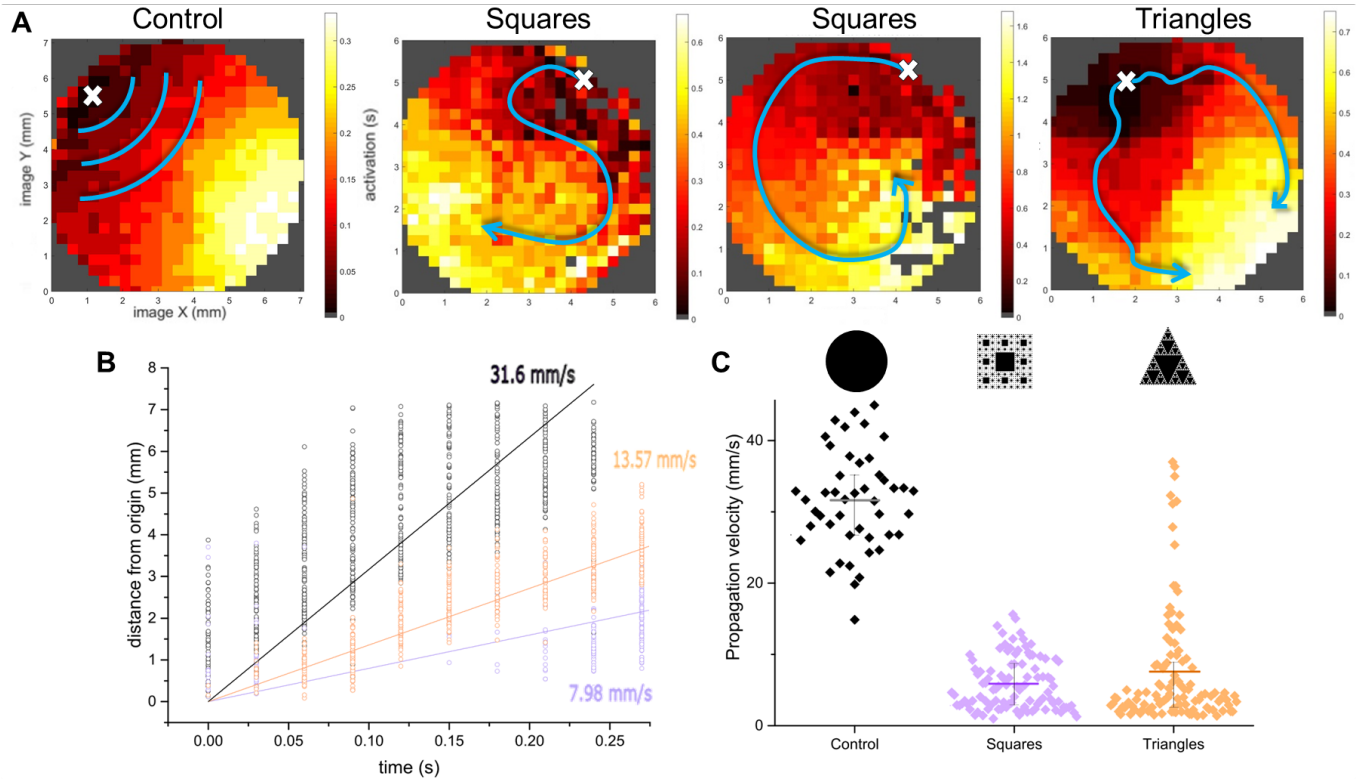

FIG. 10. **A:** Representative examples of spatio-temporal activity fronts in young cultures (DIV 6) for the control case (left), the Sierpinski square of 4th order (middle two figures) and the Sierpinski triangle of 5th order (right). Each coloured dot in the image plots is an active ROI, with the colour coded according to the activation time (black to yellow). Grey regions indicate the absence of active ROIs. The starting point of the spatio-temporal burst front is marked with a white cross and the trajectory along the culture is indicated by a blue line. **B:** Determination of the propagation velocity by linearly fitting the Euclidean distance of each ROI to the origin of activity as a function of its activation time. The data of the control case are represented in black, those belonging to the Sierpinski triangle of 5th order in orange, and those belonging to the Sierpinski square of 4th order in purple. The Pearson regression coefficients for the three cases were 0.93, 0.98, 0.97, respectively. **C:** Box plots of the propagation velocities for the three configurations: control case, Sierpinski square of 4th order, and Sierpinski triangle of 5th order. The average value and standard deviation are also represented.

nents $\alpha_1 \simeq 1.71, \beta_1 \simeq 0.59$ and $\alpha_2 \simeq 1.72, \beta_2 \simeq 0.56$ for the third and fourth order Sierpinski square respectively, and $\alpha \simeq 1.79, \beta \simeq 0.47$ for the Sierpinski triangle. As mentioned in Sec. III C, we should expect $\alpha = 1$, $\beta = 1$ for independent variables and $\alpha = 2$, $\beta = 0$ for fully correlated variables. Hence, the values obtained fall within this interval, which consistently reveals the existence of non-trivial scale-invariant correlations, which is a characteristic associated with critical systems. In addition, these exponents show a more favourable balance between both statistical behaviours compared to cultures with topography by non-fractal patterns, related to a previous work of Soriano's group [21]. This indicates that better results from a criticality perspective are obtained when fractality is incorporated.

In relation to the scaling of the covariance matrix spectrum (Fig. 11B), we obtained μ exponents of $\mu_1 \simeq 0.81$ and $\mu_2 \simeq 0.83$ for the Sierpinski squares, and $\mu \simeq 0.87$ for the Sierpinski triangle. These data showed good scaling and, more interestingly, their values were very similar to those obtained from electrophysiological data across different mouse regions, with an average of $\langle \mu \rangle = 0.84 \pm 0.14$ [29]. Therefore, with the fractal patterns it was possible to get exponents closer to the real dynamics of a mouse brain. Moreover, the covariance matrix spectrum reveals a power-law decay, suggesting the existence of a hierarchical organisation without scaling of spatio-temporal correlations which is typical of critical systems.

The exponents obtained with the fractal mature cultures (Fig. 11B upper middle) were very similar to the control case. As mentioned in Sec. IV A, they became more synchronous, thereby the possible criticality was eliminated and a worse scaling was generated.

On the other hand, it can be observed in Fig. 11C that the fractal patterns have a higher dynamic richness, as the distribution of pairwise peak count covariance values is wider, revealing the presence of heterogeneously correlated pairs in all areas. In addition, two peaks are observed which could be understood as two relevant time scales, corresponding to two different burst rates contributing to the collective dynamics. This suggests a

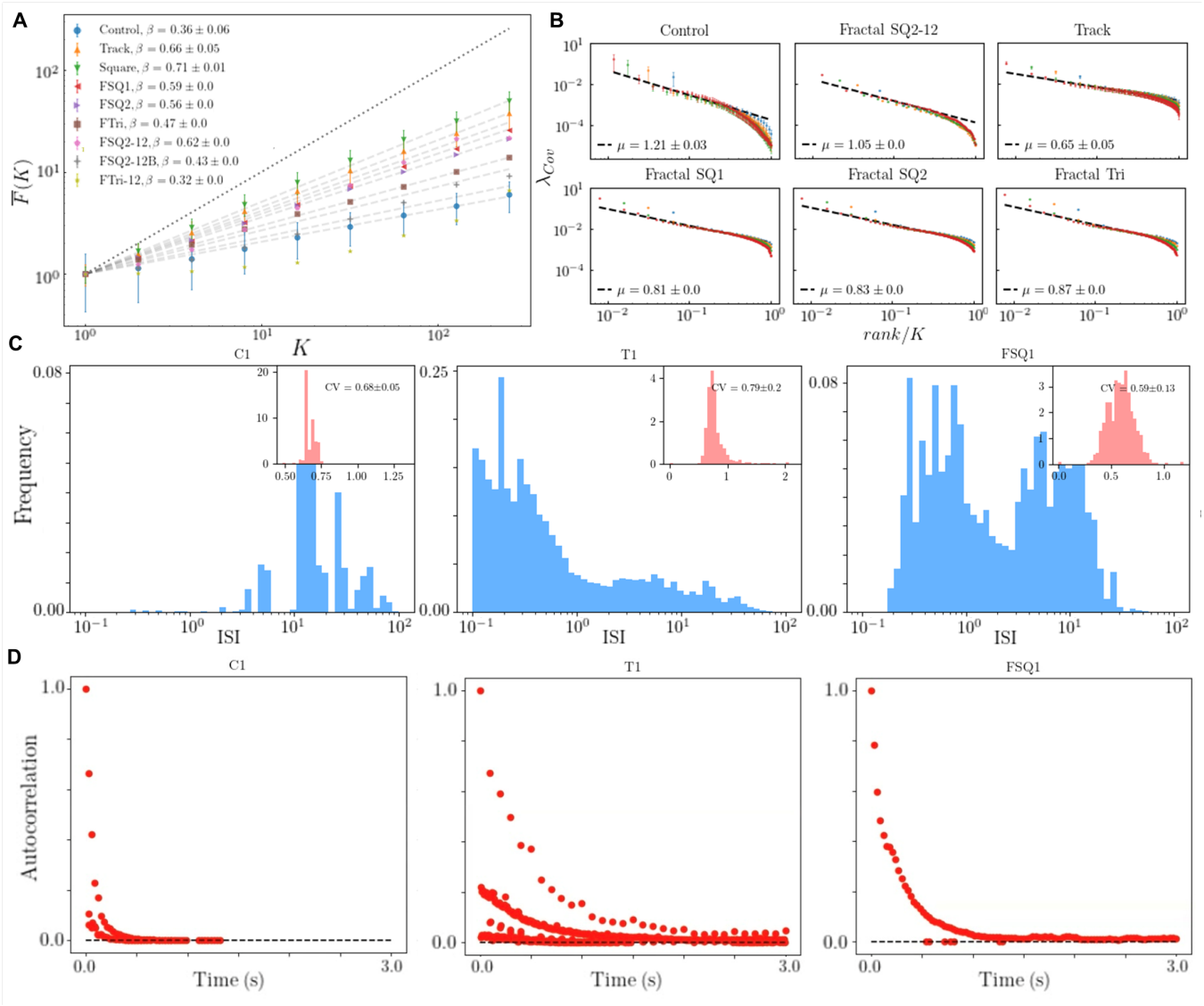

FIG. 11. Phenomenological analysis results of the renormalisation group (RG) of the neuronal culture activity with different topographical patterns. **A:** Scaling of the free energy $F(k)$, which represents the probability of being silent. The dashed line corresponds to the expected behaviour for uncorrelated variables. The legend of the plot specifies the different topographic patterns of the neuronal cultures: 'Track' and 'Square' correspond to non-fractal topographical patterns whose data was obtained from Ref. [21], FSQ1 (3rd order Sierpinski square), FSQ2 (4th order Sierpinski square), FTri (5th order Sierpinski triangle), all corresponding to DIV 6, and the last three correspond to the same fractal configurations but in DIV 12. **B:** Scaling of the covariance matrix spectrum for activity in clusters of size K = 16, 32, 64, 128 (blue, yellow, green and red markers, respectively) in different topographic patterns: Control case, 4th order Sierpinski square in DIV 12, lines, 3rd order Sierpinski square, 4th order Sierpinski square and 5th order Sierpinski triangle in DIV 6, in that order, from top to bottom and from left to right. **C:** Distribution of pairwise peak count covariance values in the control case (C1), line case (T1) and 4th order Sierpinski square in DIV 6 (FSQ1). **D:** Autocorrelations as a function of time.

scale-free hierarchical organisation in neural dynamics.

Moreover, it is worth noting that autocorrelation is an important measure, as it assesses the similarity or temporal dependence of the average activity of neurons over time. In Fig. 11D, it can be seen that due to periodic synchronisation, the correlation decays very fast (time when there is no firing) and then rises again, indicating the presence of periodic oscillations in neuronal activity (on-off behaviour). In contrast, in the fractal case, a well-defined curve can be observed, confirming the existence of a hierarchical organisation of spatio-temporal correlations typical of critical systems. In addition, the dynamics no longer follow an on-off pattern, but at the collective level there is always activity correlated with itself.

Finally, once the critical exponents have been found,

it is possible to verify whether they fulfil the hyperscale relation established in Sec. III C. By substituting the expressions $\nu_\perp = \beta/\alpha$ and $\mu = (2-\eta)/d$ into Eq. (10), it is obtained:

$$4 - d(\mu + 1) = \alpha, \tag{11}$$

where $d = 2$, since the neuronal cultures were performed on topographical quasi-flat 2d surface.

The exponents obtained experimentally are:

- **FSQ1:** $\alpha = 1,71$, $\beta = 0.59$, $\mu = 0.81$.
- **FSQ2:** $\alpha = 1,72$, $\beta = 0.56$, $\mu = 0.83$.
- **FTri:** $\alpha = 1,79$, $\beta = 0.47$, $\mu = 0.87$.

Substituting them into Eq. (11) gives:

- **FSQ1:** $4 - 2 \cdot (0.81 + 1) = 0.38 \neq 1.71$.
- **FSQ2:** $4 - 2 \cdot (0.83 + 1) = 0.34 \neq 1.72$.
- **FTri:** $4 - 2 \cdot (0.87 + 1) = 0.26 \neq 1.79$.

In this way, it can be seen that the hyperscale relation is not fulfilled, and therefore the dynamical system in question does not follow the universality class proposed by the theoretical argument based on the contact process. This lack of agreement between the experimental results and the theory could be associated with the limitations of the theoretical model, which is insufficient to fully describe the characteristics of the system under study.

D. Limitations of the study

The experimental part of this project started in November 2022, when the fractal patterns were designed. Shortly afterwards, weekly neuronal cultures using these substrates began to be performed. However, optimal results were achieved at the beginning of April due to a set of experimental difficulties. Therefore, a total of about 50 experiments were carried out, of which the last 10 were reproducible.

Which were the main problems encountered?

Firstly, there were problems with the PDMS mould, as bubbles appeared during the mixing and curing process, which negatively affected the properties and homogeneity of the PDMS. To solve this problem, a vacuum chamber was used to reduce the atmospheric pressure, allowing the bubbles trapped in the PDMS to expand and be removed.

Secondly, another problem was experienced with the curing of the PDMS, as despite following the same protocol as usual, it suddenly stopped curing properly and attached to the mould. Although an attempt was made to fix it, in the end it was necessary to repeat the photolithography process to create new wafers with the same fractal patterns. Soon after, it was discovered that the PDMS had lost its curing properties due to expiration, which meant that new PDMS had to be used.

On the other hand, it was observed that the neurons did not follow the fractal patterns, aggregated strongly, and exhibited rather synchronous dynamics. Initially, this inhomogeneity was attributed to the surface coating, so different polymers and proteins were tested to improve cell adhesion. However, it was identified that the main problem lay in the cell density, which favoured neuronal aggregation and synchronisation of activity; and in the hydrophobicity of PDMS, which made it difficult for neurons to interconnect and follow fractal patterns. To address these problems, cell density was halved and plasma treatment was carried out every week. This improvement was verified by comparing cultures with and without plasma treatment and with different densities, under the microscope and by immunostaining techniques.

Therefore, it took several months of weekly experimentation with different conditions to find the optimal conditions that would provide increased dynamic richness in the neuronal cultures. It is important to note that this increase in dynamic richness was achieved in young neuronal cultures with fractal geometry. However, the results obtained with these same cultures, but with more time *in vitro*, were more similar to standard cultures. In this way, there are still challenges in the search for more optimal results in mature neuronal cultures. This involves exploring different culture conditions, growth media and factors that promote neuronal development and maturation. In addition, electrical stimulation strategies could be implemented to modulate neuronal activity and promote more robust organisation in the cultures.

V. CONCLUSIONS

This project addressed the challenge of achieving a more realistic simulation of the brain by modifying the geometry of the substrate on which neurons are grown. Fractal patterns were used to enhance connectivity and promote richer dynamics in the cultures. In addition, the hypothesis of self-organised criticality in neuronal activity patterns was investigated, which suggests that the brain exhibits dynamics close to a critical state.

The results obtained in this study provide evidence that neuronal cultures with fractal geometry show richer and more complex dynamics compared to standard cultures, which present highly synchronous on-off behaviour. Fractal cultures were observed to exhibit more varied activation patterns, with bursts of activity of different sizes and greater spontaneous activity outside these bursts. In addition, greater variability in neuronal coactivation patterns was observed, as well as the emergence of spatiotemporal activity fronts with more diverse structures and slower propagation speeds. This phenomenon is associated with system anisotropy and reduced connectivity, leading to emergent patterns and more brain-like behaviour.

On the other hand, the renormalisation approach used in this study allowed to analyse the data in the context of criticality and to characterise the system as critical using scaling laws. The quantities of interest, such as the variance of the activity distributions, the free energy and the covariance matrix spectrum, showed specific critical exponents that support the existence of scale invariance in fractal culture dynamics. Moreover, some of these exponents showed similarities with those obtained from electrophysiological data of the mouse brain. In addition, features typical of critical systems on the edge of instability were found, such as non-trivial scale-invariant correlations and a scale-invariant hierarchical organisation of spatio-temporal correlations.

These findings demonstrate the ability of spatial constraints, represented in this case by fractal patterns, to influence the activity and functional organisation of neuronal cultures. This supports the idea that fractal geometry can enhance the ability to replicate brain dynamics and provide a more realistic experimental platform for studying the mechanisms underlying neural activity. Moreover, neuronal cultures with fractal substrates support the hypothesis of self-organised criticality in neuronal activity patterns. Therefore, this study lays the groundwork to continue in this line of work and seek further improvements in the replication of experiments and in the maintenance of culture dynamics over time.

ACKNOWLEDGMENTS

I would like to express my sincere thanks to my advisor Dr. Jordi Soriano, for his invaluable help, patience, willingness and enthusiasm throughout the development of this project. His dedication and passion in this field of research have been a constant source of inspiration. I would also like to extend my gratitude to my lab partners, Clara López-Leon, Anna-Christina Häb and Akke Mats Houben, for their valuable help, for everything they have taught me and for their unconditional support. Their collaboration has greatly enriched this project.

In addition, I would like to thank the IBEC technicians for their training in photolithography and plasma treatment processes, and the researchers Guillermo Barrios and Miguel Ángel Muñoz for their help in the criticality study.

I am also indebted to the Institute of Complex Systems of the University of Barcelona (UBICS) for having granted me a collaboration scholarship that has allowed me to develop this Master's thesis under the supervision of one of its members.

Finally, I would like to express my deep gratitude to my parents and close friends for their constant unconditional support, especially during the most difficult moments of this year.

[1] L. J. Millet and M. U. Gillette, "Over a century of neuron culture: from the hanging drop to microfluidic devices." *The Yale journal of biology and medicine*, vol. 85, no. 4, pp. 501–521, dec 2012.

[2] J. Soriano, "Neuronal cultures: Exploring biophysics, complex systems, and medicine in a dish," *Biophysica*, vol. 3, no. 1, pp. 181–202, 2023.

[3] D. R. Chialvo, "Emergent complex neural dynamics," *Nature physics*, vol. 6, no. 10, pp. 744–750, 2010.

[4] K. Heiney, O. Huse Ramstad, V. Fiskum, N. Christiansen, A. Sandvig, S. Nichele, and I. Sandvig, "Criticality, connectivity, and neural disorder: a multifaceted approach to neural computation," *Frontiers in computational neuroscience*, vol. 15, p. 611183, 2021.

[5] P. A. Rutecki, "Neuronal excitability: voltage-dependent currents and synaptic transmission." *Journal of clinical neurophysiology: official publication of the American Electroencephalographic Society*, vol. 9, no. 2, pp. 195–211, 1992.

[6] A. Meir, S. Ginsburg, A. Butkevich, S. G. Kachalsky, I. Kaiserman, R. Ahdut, S. Demirgoren, and R. Rahamimoff, "Ion channels in presynaptic nerve terminals and control of transmitter release," *Physiological reviews*, vol. 79, no. 3, pp. 1019–1088, 1999.

[7] L. Cohen, "Changes in neuron structure during action potential propagation and synaptic transmission." *Physiological reviews*, vol. 53, no. 2, pp. 373–418, 1973.

[8] A. G. Blankenship and M. B. Feller, "Mechanisms underlying spontaneous patterned activity in developing neural circuits." *Nature reviews. Neuroscience*, vol. 11, pp. 18–29, 1 2010.

[9] J. G. Orlandi, J. Soriano, E. Alvarez-Lacalle, S. Teller, and J. Casademunt, "Noise focusing and the emergence of coherent activity in neuronal cultures," *Nat. Phys.*, vol. 9, no. 9, pp. 582–590, 2013.

[10] M. D. Greicius, K. Supekar, V. Menon, and R. F. Dougherty, "Resting-state functional connectivity reflects structural connectivity in the default mode network," *Cerebral cortex*, vol. 19, no. 1, pp. 72–78, 2009.

[11] A. Ponce-Alvarez, M. L. Kringelbach, and G. Deco, "Critical scaling of whole-brain resting-state dynamics," *Communications Biology*, vol. 6, no. 1, p. 627, 2023.

[12] M. D. Fox and M. Greicius, "Clinical applications of resting state functional connectivity," *Frontiers in systems neuroscience*, p. 19, 2010.

[13] K. J. Friston, "Functional and effective connectivity: A review," *Brain Connectivity*, vol. 1, pp. 13–36, 1 2011.

[14] H. E. Wang, C. G. Bénar, P. P. Quilichini, K. J. Friston, V. K. Jirsa, and C. Bernard, "A systematic framework for functional connectivity measures," *Frontiers in Neuroscience*, vol. 8, p. article 405, 2014.

[15] E. A. Variano, J. H. McCoy, and H. Lipson, "Networks, dynamics, and modularity," *Physical review letters*, vol. 92, p. 188701, 5 2004.

[16] O. Sporns and R. F. Betzel, "Modular brain networks," *Annual Review of Psychology*, vol. 67, pp. 613–640, 2016.

[17] H. Yamamoto, S. Moriya, K. Ide, T. Hayakawa, H. Akima, S. Sato, S. Kubota, T. Tanii, M. Niwano, S. Teller, J. Soriano, and A. Hirano-Iwata, "Impact of modular organization on dynamical richness in cortical networks," *Science Advances*, vol. 4, p. eaau4914, 2018.

[18] G. Zamora-López, C. Zhou, and J. Kurths, "Exploring brain function from anatomical connectivity," *Frontiers in neuroscience*, vol. 5, p. 83, 2011.

[19] O. Sporns, "Network attributes for segregation and integration in the human brain," *Current opinion in neurobiology*, vol. 23, no. 2, pp. 162–171, 2013.

[20] E. Tibau, M. Valencia, and J. Soriano, "Identification of neuronal network properties from the spectral analysis of calcium imaging signals in neuronal cultures," *Front. Neur. Circ.*, vol. 7, p. article 199, 2013.

[21] M. Montalà-Flaquer, C. F. López-León, D. Tornero, A. M. Houben, T. Fardet, P. Monceau, S. Bottani, and J. Soriano, "Rich dynamics and functional organization on topographically designed neuronal networks in vitro," *iScience*, vol. 25, p. article 105680, 12 2022.

[22] J. M. Beggs and N. Timme, "Being critical of criticality in the brain," *Frontiers in physiology*, vol. 3, p. 163, 2012.

[23] L. Cocchi, L. L. Gollo, A. Zalesky, and M. Breakspear, "Criticality in the brain: A synthesis of neurobiology, models and cognition," *Progress in neurobiology*, vol. 158, pp. 132–152, 2017.

[24] P. Moretti and M. A. Muñoz, "Griffiths phases and the stretching of criticality in brain networks," *Nature communications*, vol. 4, no. 1, p. 2521, 2013.

[25] M. Yaghoubi, T. de Graaf, J. G. Orlandi, F. Girotto, M. A. Colicos, and J. Davidsen, "Neuronal avalanche dynamics indicates different universality classes in neuronal cultures," *Scientific reports*, vol. 8, no. 1, p. 3417, 2018.

[26] J. P. Sethna, K. A. Dahmen, and C. R. Myers, "Crackling noise," *Nature*, vol. 410, no. 6825, pp. 242–250, 2001.

[27] K. Christensen and N. Moloney, "Complexity and criticality, vol. 1 london," *UK: Imperial College Press*, 2005.

[28] G. Nicoletti, S. Suweis, and A. Maritan, "Scaling and criticality in a phenomenological renormalization group," *Physical Review Research*, vol. 2, no. 2, p. 023144, 2020.

[29] G. B. Morales, S. Di Santo, and M. A. Muñoz, "Quasi-universal scaling in mouse-brain neuronal activity stems from edge-of-instability critical dynamics," *Proceedings of the National Academy of Sciences*, vol. 120, no. 9, p. e2208998120, 2023.

[30] S. Okujeni, S. Kandler, and U. Egert, "Mesoscale architecture shapes initiation and richness of spontaneous network activity," *The Journal of Neuroscience*, vol. 37, p. 3972–3987, 2017.

[31] M. Rubinov and O. Sporns, "Complex network measures of brain connectivity: uses and interpretations." *NeuroImage*, vol. 52, no. 3, pp. 1059–1069, sep 2010.

[32] M. Shein-Idelson, E. Ben-Jacob, and Y. Hanein, "Engineered neuronal circuits: a new platform for studying the role of modular topology," *Frontiers in neuroengineering*, vol. 4, p. 10, 2011.

[33] P. Nikolakopoulou, R. Rauti, D. Voulgaris, I. Shlomy, B. M. Maoz, and A. Herland, "Recent progress in translational engineered in vitro models of the central nervous system," *Brain*, vol. 143, no. 11, pp. 3181–3213, 2021.

[34] D. S. Bassett and E. T. Bullmore, "Human brain networks in health and disease." *Current opinion in neurology*, vol. 22, no. 4, pp. 340–347, aug 2009.

[35] C. J. Stam, "Modern network science of neurological disorders," *Nature Reviews Neuroscience*, vol. 15, no. 10, pp. 683–695, sep 2014.

[36] J. G. Orlandi, S. Fernández-García, A. Comella-Bolla, M. Masana, G. G.-D. Barriga, M. Yaghoubi, A. Kipp, J. M. Canals, M. A. Colicos, J. Davidsen, J. Alberch, and J. Soriano, "Netcal: an interactive platform for large-scale, network and population dynamics analysis of calcium imaging recordings," *Zenodo.org. Version 7.0 beta.*, 2017.

[37] G. Zamora-López, Y. Chen, G. Deco, M. L. Kringelbach, and C. Zhou, "Functional complexity emerging from anatomical constraints in the brain: The significance of network modularity and rich-clubs," *Scientific Reports*, vol. 6, pp. 1–18, 2016.

[38] R. Dickman and M. M. de Oliveira, "Quasi-stationary simulation of the contact process," *Physica A: Statistical Mechanics and its Applications*, vol. 357, no. 1, pp. 134–141, 2005.